Cai, C., Montens, S. "Wind Effects on Long-Span Bridges."
Bridge Engineering Handbook.
Ed. Wai-Fah Chen and Lian Duan
Boca Raton: CRC Press, 2000

57

Wind Effects on Long-Span Bridges

Chun S. Cai
Florida Department of Transportation

Serge Montens
Jean Muller International, France

57.1 Introduction

The development of modern materials and construction techniques has resulted in a new generation of lightweight flexible structures. Such structures are susceptible to the action of winds. Suspension bridges and cable-stayed bridges shown in Figure 57.1 are typical structures susceptible to wind-induced problems.

The most renowned bridge collapse due to winds is the Tacoma Narrows suspension bridge linking the Olympic Peninsula with the rest of the state of Washington. It was completed and opened to traffic on July 1, 1940. Its 853-m main suspension span was the third longest in the world. This bridge became famous for its serious wind-induced problems that began to occur soon after it opened. "Even in winds of only 3 to 4 miles per hour, the center span would rise and fall as much as four feet…, and drivers would go out of their way either to avoid it or cross it for the roller coaster thrill of the trip. People said you saw the lights of cars ahead disappearing and reappearing as they bounced up and down. Engineers monitored the bridge closely but concluded that the motions were predictable and tolerable" [1].

On November 7, 1940, 4 months and 6 days after the bridge was opened, the deck oscillated through large displacements in the vertical vibration modes at a wind velocity of about 68 km/h. The motion changed to a torsional mode about 45 min later. Finally, some key structural members became overstressed and the main span collapsed.

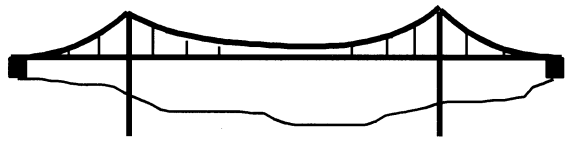

Suspension Bridge

Cable-Stayed Bridge

FIGURE 57.1 Typical wind-sensitive bridges.

Some bridges were destroyed by wind action prior to the failure of the Tacoma Narrows bridge. However, it was this failure that shocked and intrigued bridge engineers to conduct scientific investigations of bridge aerodynamics. Some existing bridges, such as the Golden Gate suspension bridge in California with a main span of 1280 m, have also experienced large wind-induced oscillations, although not to the point of collapse. In 1953, the Golden Gate bridge was stiffened against aerodynamic action [2].

Wind-induced vibration is one of the main concerns in a long-span bridge design. This chapter will give a brief description of wind-induced bridge vibrations, experimental and theoretical solutions, and state-of-the-art applications.

57.2 Winds and Long-Span Bridges

57.2.1 Description of Wind at Bridge Site

The atmospheric wind is caused by temperature differentials resulting from solar radiations. When the wind blows near the ground, it is retarded by obstructions making the mean velocity at the ground surface zero. This zero-velocity layer retards the layer above and this process continues until the wind velocity becomes constant. The distance between the ground surface and the height of constant wind velocity varies between 300 m and 1 km. This 1-km layer is referred to as the boundary layer in which the wind is turbulent due to its interaction with surface friction. The variation of the mean wind velocity with height above ground usually follows a logarithmic or exponential law.

The velocity of boundary wind is defined by three components: the along-wind component consisting of the mean wind velocity, $\overline{U}$, plus the turbulent component $u(t)$, the cross-wind turbulent component $v(t)$, and the vertical turbulent component $w(t)$. The turbulence is described in terms of turbulence intensity, integral length, and spectrum [3].

The turbulence intensity I is defined as

$$I = \frac{\sigma}{\overline{U}} \tag{57.1}$$

where σ = the standard deviation of wind component $u(t)$, $v(t)$, or $w(t)$; $\overline{U}$ = the mean wind velocity.

Integral length of turbulence is a measurement of the average size of turbulent eddies in the flow. There are a total of nine integral lengths (three for each turbulent component). For example, the integral length of $u(t)$ in the x-direction is defined as

$$L_u^x = \frac{1}{\sigma_u^2} \int_0^\infty R_{u1u2}(x)dx \tag{57.2}$$

where $R_{u1u2}(x)$ = cross-covariance function of $u(t)$ for a spatial distance x.

The wind spectrum is a description of wind energy vs. wind frequencies. The von Karman spectrum is given in dimensionless form as

$$\frac{nS(n)}{\sigma^2} = \frac{4\dfrac{nL}{\overline{U}}}{\left[1 + 70.8\left(\dfrac{nL}{\overline{U}}\right)^2\right]^{5/6}} \tag{57.3}$$

where n = frequency (Hz); S = autospectrum; and L = integral length of turbulence. The integral length of turbulence is not easily obtained. It is usually estimated by curve fitting the spectrum model with the measured field data.

57.2.2 Long-Span Bridge Responses to Wind

Wind may induce instability and excessive vibration in long-span bridges. Instability is the onset of an infinite displacement granted by a linear solution technique. Actually, displacement is limited by structural nonlinearities. Vibration is a cyclic movement induced by dynamic effects. Since both instability and vibration failures in reality occur at finite displacement, it is often hard to judge whether a structure failed due to instability or excessive vibration-induced damage to some key elements.

Instability caused by the interaction between moving air and a structure is termed aeroelastic or aerodynamic instability. The term *aeroelastic* emphasizes the behavior of deformed bodies, and *aerodynamic* emphasizes the vibration of rigid bodies. Since many problems involve both deformation and vibration, these two terms are used interchangeably hereafter. Aerodynamic instabilities of bridges include divergence, galloping, and flutter. Typical wind-induced vibrations consist of vortex shedding and buffeting. These types of instability and vibration may occur alone or in combination. For example, a structure must experience vibration to some extent before flutter instability starts.

The interaction between the bridge vibration and wind results in two kinds of forces: motion-dependent and motion-independent. The former vanishes if the structures are rigidly fixed. The latter, being purely dependent on the wind characteristics and section geometry, exists whether or not the bridge is moving. The aerodynamic equation of motion is expressed in the following general form:

$$[M]\{\ddot{Y}\} + [C]\{\dot{Y}\} + [K]\{Y\} = \{F(Y)\}_{md} + \{F\}_{mi} \tag{57.4}$$

where $[M]$ = mass matrix; $[C]$ = damping matrix; $[K]$ = stiffness matrix; $\{Y\}$ = displacement vector; $\{F(Y)\}_{md}$ = motion-dependent aerodynamic force vector; and $\{F\}_{mi}$ = motion-independent wind force vector.

The motion-dependent force causes aerodynamic instability and the motion-independent part together with the motion-dependent part causes deformation. The difference between short-span and long-span bridge lies in the motion-dependent part. For the short-span bridges, the motion-dependent part is insignificant and there is no concern about aerodynamic instability. For flexible structures like long-span bridges, however, both instability and vibration need to be carefully investigated.

57.3 Experimental Investigation

Wind tunnel testing is commonly used for "wind-sensitive" bridges such as cable-stayed bridges, suspension bridges, and other bridges with span lengths or structure types significantly outside of

the common ranges. The objective of a wind tunnel test is to determine the susceptibility of the bridges to various aerodynamic phenomena.

The bridge aerodynamic behavior is controlled by two types of parameters, i.e., structural and aerodynamic. The structural parameters are the bridge layout, boundary condition, member stiffness, natural modes, and frequencies. The aerodynamic parameters are wind climate, bridge section shape, and details. The design engineers need to provide all the information to the wind specialist to conduct the testing and analysis.

57.3.1 Scaling Principle

In a typical structural test, a prototype structure is scaled down to a scale model according to mass, stiffness, damping, and other parameters. In testing, the wind blows in different vertical angles (attack angles) or horizontal angles (skew angles) to cover the worst case at the bridge site. To obtain reliable information from a test, similarity must be maintained between the specimen and the prototype structure. The geometric scale λ_L, a basic parameter which is controlled by the size of an available wind tunnel, is denoted as the ratio of the dimensions of model (B_m) to the dimensions of prototype bridge (B_p) as [4]

$$\lambda_L = \frac{B_m}{B_p} \tag{57.5}$$

where subscripts m and p indicate model and prototype, respectively.

To maintain the same Froude number for both scale model and prototype bridge requires,

$$\left(\frac{U^2}{Bg}\right)_m = \left(\frac{U^2}{Bg}\right)_p \tag{57.6}$$

where g is the air gravity, which is the same for the model and prototype bridge. From Eqs. (57.5) and (57.6) we have the wind velocity scale λ_v as

$$\lambda_V = \frac{U_m}{U_p} = \sqrt{\lambda_L} \tag{57.7}$$

Reynolds number equivalence requires

$$\left(\frac{\rho UB}{\mu}\right)_m = \left(\frac{\rho UB}{\mu}\right)_p \tag{57.8}$$

where μ = viscosity and ρ = wind mass density. Equations (57.5) and (57.8) give the wind velocity scale as

$$\lambda_V = \frac{1}{\lambda_L} \tag{57.9}$$

which contradicts Eq. (57.7). It is therefore impossible in model scaling to satisfy both the Froude number equivalence and Reynolds number equivalence simultaneously. For bluff bodies such as bridge decks, flow separation is caused by sharp edges and, therefore, the Reynolds number is not important except it is too small. The too-small Reynolds number can be avoided by careful selection of λ_L. Therefore, the Reynolds number equivalence is usually sacrificed and Froude number equivalence is maintained.

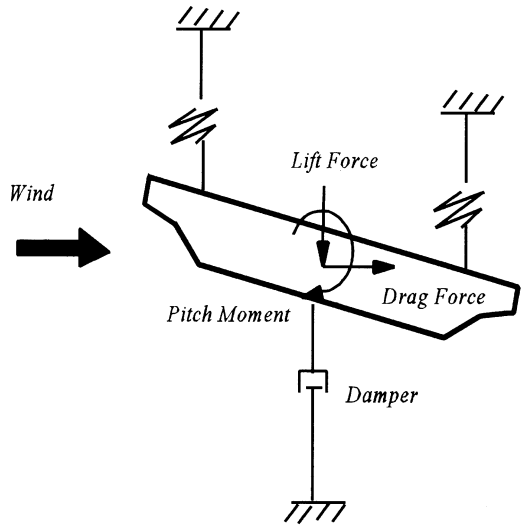

FIGURE 57.2 End view of section model.

To apply the flutter derivative information to the prototype analysis, nondimensional reduced velocity must be the same, i.e.,

$$\left(\frac{U}{NB}\right)_m = \left(\frac{U}{NB}\right)_p \tag{57.10}$$

Solving Eqs. (57.5), (57.7) and (57.10) gives the natural frequency scale as

$$\lambda_N = \frac{N_m}{N_p} = \frac{1}{\sqrt{\lambda_L}} \tag{57.11}$$

The above equivalence of reduced velocity between the section model and prototype bridge is the basis to use the section model information to prototype bridge analysis. Therefore, it should be strictly satisfied.

57.3.2 Section model

A typical section model represents a unit length of a prototype deck with a scale from 1:25 to 1:100. It is usually constructed from materials such as steel, wood, or aluminum to simulate the scaled mass and moment of inertia about the center of gravity. The section model represents only the outside shape (aerodynamic shape) of the deck. The stiffness and the vibration characteristics are represented by the spring supports.

By rigidly mounding the section in the wind tunnel, the static wind forces, such as lift, drag, and pitch moment, can be measured. To measure the aerodynamic parameters such as the flutter derivatives, the section model is supported by a spring system and connected to a damping source as shown in Figure 57.2. The spring system can be adjusted to simulate the deck stiffness in vertical and torsional directions, and therefore simulate the natural frequencies of the bridges. The damping characteristics are also adjustable to simulate different damping.

A section model is less expensive and easier to conduct than a full model. It is thus widely used in (1) the preliminary study to find the best shape of a bridge deck; (2) to identify the potential wind-induced problems such as vortex-shedding, flutter, and galloping and to guide a more-sophisticated

full model study; (3) to measure wind data, such as flutter derivatives, static force coefficients for analytical prediction of actual bridge behavior; and (4) to model some less important bridges for which a full model test cannot be economically justified.

57.3.3 Full Bridge Model

A full bridge model, representing the entire bridge or a few spans, is also called an aeroelastic model since the aeroelastic deformation is reflected in the full model test. The deck, towers, and cables are built according to the scaled stiffness of the prototype bridge. The scale of a full bridge model is usually from 1:100 to 1:300 to fit the model in the wind tunnel. The full model test is used for checking many kinds of aerodynamic phenomena and determining the wind loading on bridges.

A full bridge model is more expensive and difficult to build than a section model. It is used only for large bridges at the final design stage, particularly to check the aerodynamics of the construction phase. However, a full model test has many advantages over a section model: (1) it simulates the three-dimensional and local topographical effects; (2) it reflects the interaction between vibration modes; (3) wind effects can be directly visualized at the construction and service stages; and (4) it is more educational to the design engineers to improve the design.

57.3.4 Taut Strip Model

For this model, taut strings or tubes are used to simulate the stiffness and dynamic characteristics of the bridge such as the natural frequencies and mode shapes for vertical and torsional vibrations. A rigid model of the deck is mounted on the taut strings. This model allows, for example, to represent the main span of a deck. The taut strip model falls between section model and full model with respect to cost and reliability. For less important bridges, the taut strip model is a sufficient and economical choice. The taut strip model is used to determine critical wind velocity for vortex shedding, flutter, and galloping and displacement and acceleration under smooth or turbulent winds.

57.4 Analytical Solutions

57.4.1 Vortex Shedding

Vortex shedding is a wake-induced effect occurring on bluff bodies such as bridge decks and pylons. Wind flowing against a bluff body forms a stream of alternating vortices called a von Karman vortex street shown in Figure 57.3a. Alternating shedding of vortices creates an alternative force in a direction normal to the wind flow. This alternative force induces vibration. The shedding frequency of vortices from one surface, in either torsion or lift, can be described in terms of a nondimensional Strouhal number, S, as

$$S = \frac{ND}{\overline{U}} \tag{57.12}$$

where N = shedding frequency and D = characteristic dimension such as the diameter of a circular section or depth of a deck.

The Strouhal number (ranging from 0.05 to 0.2 for bridge decks) is a constant for a given section geometry and details. Therefore, the shedding frequency (N) increases with the wind velocity to maintain a constant Strouhal value (S). The bridge vibrates strongly but self-limited when the frequency of vortex shedding is close to one of the natural frequencies of a bridge, say, N_1 as shown in Figure 57.3. This phenomenon is called lock-in and the corresponding wind velocity is called critical velocity of vortex shedding.

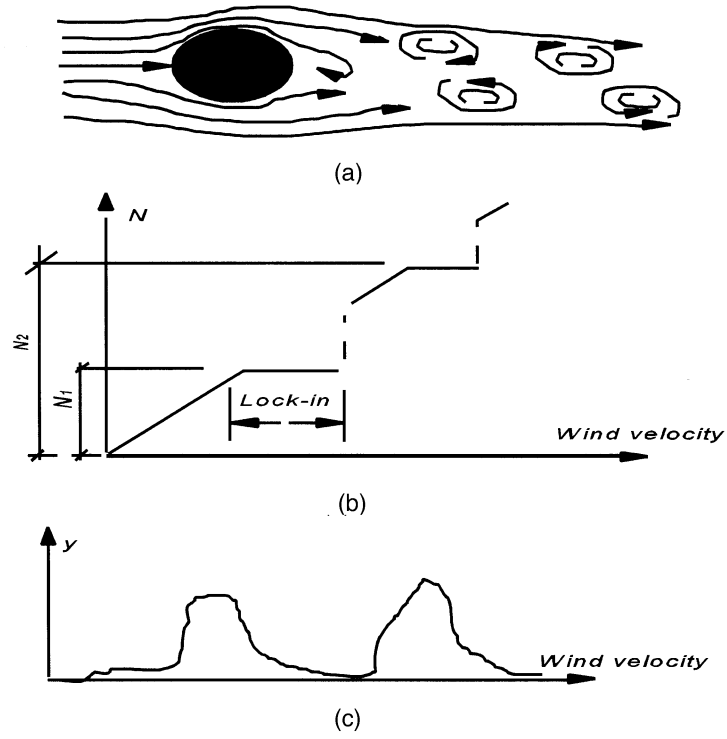

FIGURE 57.3 Explanation of vortex shedding. (a) Von Karman Street; (b) lock-in phenomenon; (c) bridge vibration

The lock-in occurs over a small range of wind velocity within which the Strouhal relation is violated since the increasing wind velocity and a fixed shedding frequency results in a decreasing Strouhal number. The bridge natural frequency, not the wind velocity, controls the shedding frequency. As wind velocity increases, the lock-in phenomenon disappears and the vibration reduces to a small amplitude. The shedding frequency may lock in another higher natural frequency (N_2) at higher wind velocity. Therefore, many wind velocities cause vortex shedding.

To describe the above experimental observation, much effort has been made to find an expression for forces resulting from vortex shedding. Since the interaction between the wind and the structure is very complex, no completely successful model has yet been developed for bridge sections. Most models deal with the interaction of wind with circular sections. A semiempirical model for the lock-in is given as [3]

$$m\ddot{y} + c\dot{y} + ky = \frac{1}{2}\rho U^2(2D)\left[Y_1(K)\left(1-\varepsilon\frac{y^2}{D^2}\right)\frac{\dot{y}}{D} + Y_2(K)\frac{y}{D} + \frac{1}{2}C_L(K)\sin(\omega t+\phi)\right] \qquad (57.13)$$

where $k = B\omega/\overline{U}$ = reduced frequency; Y_1, Y_2, ε, and C_L = parameters to be determined from experimental observations. The first two terms of the right side account for the motion-dependent force. More particularly, the $\dot{y}$ term accounts for aerodynamic damping and y term for aerodynamic stiffness. The ε accounts for the nonlinear aerodynamic damping to ensure the self-limiting nature of vortex shedding. The last term represents the instantaneous force from vortex shedding alone which is sinusoidal with the natural frequency of bridge. Solving the above equation gives the vibration y.

Vortex shedding occurs in both laminar and turbulent flow. According to some experimental observations, turbulence helps to break up vortices and therefore helps to suppress the vortex shedding response. A more complete analytical model must consider the interaction between modes, the spanwise correlation of aerodynamic forces and the effect of turbulence.

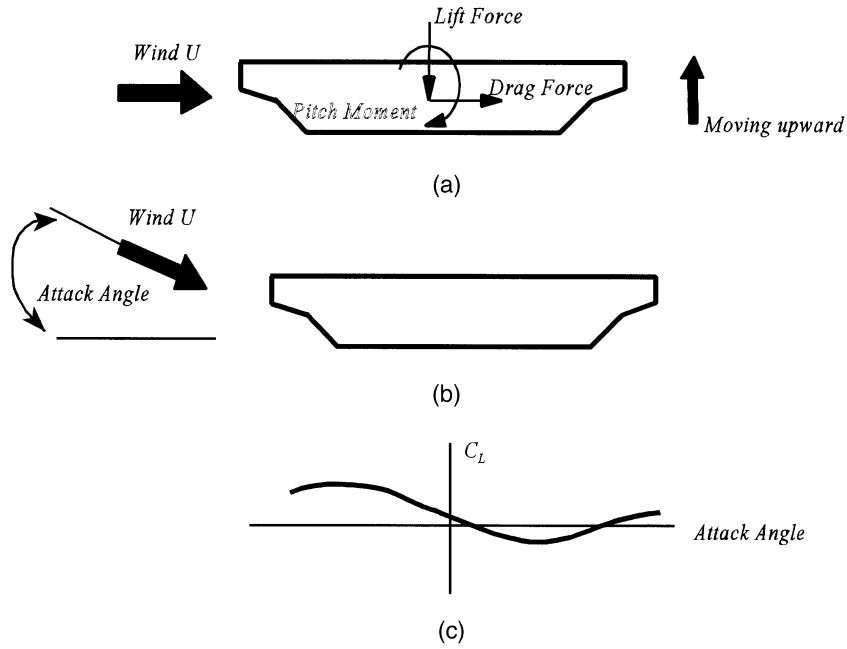

FIGURE 57.4 Explanation of galloping. (a) Section moving upward; (b) motionless section with a wind attack angle; (c) static force coefficient vs. attack angle.

For a given section shape with a known Strouhal number and natural frequencies, the lock-in wind velocities can be calculated with Eq. (57.12). The calculated lock-in wind velocities are usually lower than the maximum wind velocity at bridge sites. Therefore, vortex shedding is an inevitable aerodynamic phenomenon. However, vibration excited by vortex shedding is self-limited because of its nonlinear nature. A relatively small damping is often sufficient to eliminate, or at least reduce, the vibrations to acceptable limits.

Although there are no acceptance criteria for vortex shedding in the design specifications and codes in the United States, there is a common agreement that limiting acceleration is more appropriate than limiting deformation. It is usually suggested that the acceleration of vortex shedding is limited to 5% of gravity acceleration when wind speed is less than 50 km/h and 10% of gravity acceleration when wind speed is higher. The acceleration limitation is then transformed into the displacement limitation for a particular bridge.

57.4.2 Galloping

Consider that in Figure 57.4 (a) a bridge deck is moving upward with a velocity $\dot{y}$ under a horizontal wind U. This is equivalent to the case of Figure 57.4b that the deck is motionless and the wind blows downward with an attack angle α ($\tan(\alpha) = \dot{y}/U$). If the measured static force coefficient of this case is negative (upward), then the deck section will be pushed upward further resulting in a divergent vibration or galloping. Otherwise, the vibration is stable. Galloping is caused by a change in the effective attack angle due to vertical or torsional motion of the structure. A negative slope in the plot of either static lift or pitch moment coefficient vs. the angle of attack, shown in Figure 57.4c, usually implies a tendency for galloping. Galloping depends mainly on the quasi-steady behavior of the structure.

The equation of motion describing this phenomenon is

$$m\ddot{y} + c\dot{y} + ky = -\frac{1}{2}\rho U^2 B\left(\frac{dC_L}{d\alpha} + C_D\right)_{\alpha=0}\frac{\dot{y}}{U} \tag{57.14}$$

The right side represents the aerodynamic damping and C_L and C_D are static force coefficients in the lift and drag directions, respectively. If the total damping is less than zero, i.e.,

$$c + \frac{1}{2}\rho UB\left(\frac{dC_L}{d\alpha} + C_D\right)_{\alpha=0} \le 0 \tag{57.15}$$

then the system tends toward instability. Solving the above equation gives the critical wind velocity for galloping. Since the mechanical damping c is positive, the above situation is possible only if the following Den Hartog criterion [5] is satisfied

$$\left(\frac{dC_L}{d\alpha} + C_D\right)_{\alpha=0} \le 0 \tag{57.16}$$

Therefore, a wind tunnel test is usually conducted to check against Eq. (57.16) and to make necessary improvement of the section to eliminate the negative tendency for the possible wind velocity at a bridge site.

Galloping rarely occurs in highway bridges, but noted examples are pedestrian bridges, pipe bridges, and ice-coated cables in power lines. There are two kinds of cable galloping: cross-wind galloping, which creates large-amplitude oscillations in a direction normal to the flow, and wake galloping caused by the wake shedding of the upwind structure.

57.4.3 Flutter

Flutter is one of the earliest recognized and most dangerous aeroelastic phenomena in airfoils. It is created by self-excited forces that depend on motion. If a system immersed in wind flow is given a small disturbance, its motion will either decay or diverge depending on whether the energy extracted from the flow is smaller or larger than the energy dissipated by mechanical damping. The theoretical line dividing decaying and diverging motions is called the critical condition. The corresponding wind velocity is called the critical wind velocity for flutter or simply the flutter velocity at which the motion of the bridge deck tends to grow exponentially as shown in Figure 57.5a.

When flutter occurs, the oscillatory motions of all degrees of freedom in the structure couple to create a single frequency called the flutter frequency. Flutter is an instability phenomenon; once it takes place, the displacement is infinite by linear theory. Flutter may occur in both laminar and turbulent flows.

The self-excited forces acting on a unit deck length are usually expressed as a function of the flutter derivatives. The general format of the self-excited forces written in matrix form [2,6] for finite element analysis is

$$\begin{Bmatrix} L_{se} \\ D_{se} \\ M_{se} \end{Bmatrix} = \frac{1}{2}\rho U^2(2B)\left(\begin{bmatrix} \frac{k^2H_4^*}{B} & \frac{k^2H_6^*}{B} & k^2H_3^* \\ \frac{k^2P_4^*}{B} & \frac{k^2P_6^*}{B} & k^2P_3^* \\ k^2A_4^* & k^2A_6^* & k^2A_3^*B \end{bmatrix}\begin{Bmatrix} h \\ p \\ \alpha \end{Bmatrix} + \begin{bmatrix} \frac{kH_1^*}{\bar{U}} & \frac{kH_5^*}{\bar{U}} & \frac{kH_2^*B}{\bar{U}} \\ \frac{kP_1^*}{\bar{U}} & \frac{kP_5^*}{\bar{U}} & \frac{kP_2^*B}{\bar{U}} \\ \frac{kA_1^*B}{\bar{U}} & \frac{kA_5^*B}{\bar{U}} & \frac{kA_2^*B^2}{\bar{U}} \end{bmatrix}\begin{Bmatrix} \dot{h} \\ \dot{p} \\ \dot{\alpha} \end{Bmatrix}\right) \tag{57.17}$$

$$= U^2\left[F_d\right]\{q\} + U^2\left[F_v\right]\{\dot{q}\}$$

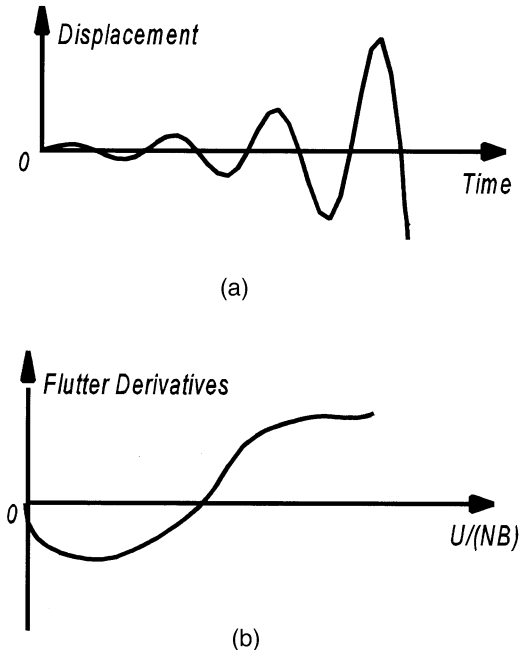

FIGURE 57.5 Explanation of flutter. (a) Bridge flutter vibration; (b) typical flutter derivations.

where L_{se}, D_{se}, and M_{se} = self-excited lift force, drag force, and pitch moment, respectively; h, p, and α = displacements at the center of a deck in the directions corresponding to L_{se}, D_{se}, and M_{se}, respectively; ρ = mass density of air; B = deck width; H_i^*, P_i^*, and A_i^* (i = 1 to 6) = generalized flutter derivatives; $k = B\omega/\overline{U}$ = reduced frequency; ω = oscillation circular frequency; $\overline{U}$ = mean wind velocity; and $[F_d]$ and $[F_v]$ = flutter derivative matrices corresponding to displacement and velocity, respectively.

While the flutter derivatives H_i^* and A_i^* have been experimentally determined for i = 1 to 4, the term P_i^* is theoretically derived in state-of-the-art applications. The other flutter derivatives (for i = 5 and 6) have been neglected in state-of-the-art analysis.

In linear analyses, the general aerodynamic motion equations of bridge systems are expressed in terms of the generalized mode shape coordinate $\{\xi\}$

$$[M^*]\{\ddot{\xi}\} + ([D^*] - U^2[AD^*])\{\dot{\xi}\} + ([K^*] - U^2[AS^*])\{\xi\} = 0 \tag{57.18}$$

where $[M^*]$, $[D^*]$, and $[K^*]$ = generalized mass, damping, and stiffness matrices, respectively; and $[AS^*]$ and $[AD^*]$ = generalized aerodynamic stiffness and aerodynamic damping matrices, respectively. Matrices $[M^*]$, $[D^*]$, and $[K^*]$ are derived the same way as in the general dynamic analysis. Matrices $[AS^*]$ and $[AD^*]$, corresponding to $[F_d]$ and $[F_v]$ in Eq. (57.17), respectively, are assembled from aerodynamic element forces. It is noted that even the structural and dynamic matrices $[K^*]$, $[M^*]$, and $[D^*]$ are uncoupled between modes, the motion equation is always coupled due to the coupling of aerodynamic matrices $[AS^*]$ and $[AD^*]$.

Flutter velocity, U, and flutter frequency, ω, are obtained from the nontrivial solution of Eq. (57.18) as

$$\left|\left(-\omega^2[M^*] + [K^*] - \overline{U}^2[AS^*] + \omega([D^*] - \overline{U}^2[AD^*])\, i\right)\right| = 0 \tag{57.19}$$

For a simplified uncoupled single degree of freedom, the above equation reduces to

$$\omega^2 = \frac{[K^*] - \overline{U}^2[AS^*]}{[M^*]} \tag{57.20}$$

and

$$U_{cr}^2 = \frac{[D^*]}{[AD^*]} \tag{57.21}$$

Since the aerodynamic force $[AS^*]$ is relatively small, it can be seen that the flutter frequency in Eq. (57.20) is close to the natural frequency $[K^*]/[M^*]$. Equation (57.21) can be also derived from Eq. (57.18) as the zero-damping condition. Zero-damping cannot occur unless $[AD^*]$ is positive. The value of $[AD^*]$ depends on the flutter derivatives. An examination of the flutter derivatives gives a preliminary judgment of the flutter behavior of the section. Necessary section modifications should be made to eliminate the positive flutter derivatives as shown in Figure 57.5b, especially the A_2^* and H_1^*. The A_2^* controls the torsional flutter and the H_1^* controls the vertical flutter. It can be seen from Eq. (57.21) that an increase in the mechanical damping $[D^*]$ increases the flutter velocity. It should be noted that for a coupled flutter, zero-damping is a sufficient but not a necessary condition.

A coupled flutter is also called stiffness-driven or classical flutter. An uncoupled flutter is called damping-driven flutter since it is caused by zero-damping. Since flutter of a suspension bridge is usually controlled by its first torsional mode, the terminology *flutter* was historically used for a torsional aerodynamic instability. Vertical aerodynamic instability is traditionally treated in a quasi-static approach, i.e., as is galloping. In recent literature, flutter is any kind of aerodynamic instability due to self-excited forces, whether vertical, torsional, or coupled vibrations.

Turbulence is assumed beneficial for flutter stability and is usually ignored. Some studies include turbulence effect by treating along-wind velocity U as mean velocity, $\overline{U}$, plus a turbulent component, $u(t)$. The random nature of $u(t)$ results in an equation of random damping and stiffness. Complicated mathematics, such as stochastic differentiation, need to be involved to solve the equation [7].

Time history and nonlinear analyses can be conducted on Eq. (57.18) to investigate postflutter behavior and to include the effects of both geometric and material nonlinearities. However, this is not necessary for most practical applications.

57.4.4 Buffeting

Buffeting is defined as the forced response of a structure to random wind and can only take place in turbulent flows. Turbulence resulting from topographical or structural obstructions is called oncoming turbulence. Turbulence induced by bridge itself is called signature turbulence. Since the frequencies of signature turbulence are generally several times higher than the important natural frequencies of the bridge, its effect on buffeting response is usually small.

Buffeting is a random vibration problem of limited displacement. The effects of buffeting and vortex shedding are similar, except that vibration is random in the former and periodic in the latter. Both buffeting and vortex shedding influence bridge service behavior and may result in fatigue damage that could lead to a eventual collapse of a bridge. Buffeting also influences ultimate strength behavior.

Similar to Eq. (57.17), the buffeting forces are expressed in the matrix form [2] for finite element analysis as

$$\begin{Bmatrix} L_b \\ D_b \\ M_b \end{Bmatrix} = \frac{1}{2}\rho \bar{U}^2 B \begin{bmatrix} 2C_L & \left(\frac{dC_L}{d\alpha} + C_D\right) \\ 2C_D & \frac{dC_D}{d\alpha} \\ 2C_M B & \frac{dC_M}{d\alpha} B \end{bmatrix} \begin{Bmatrix} \frac{u(t)}{\bar{U}} \\ \frac{w(t)}{\bar{U}} \end{Bmatrix} = \bar{U}^2 [C_b] \{\eta\} \tag{57.22}$$

where C_D, C_L, and C_M = static aerodynamic coefficients for drag, lift, and pitch moment, respectively; α = angle of wind attack; $[C_b]$ = static coefficient matrix; and $\{\eta\}$ = vector of turbulent wind components normalized by mean wind velocity.

The equation of motion for buffeting is similar to Eq. (57.18), but with one more random buffeting force as

$$[M^*]\{\ddot{\xi}\} + ([D^*] - U^2[AD^*])\{\dot{\xi}\} + ([K^*] - U^2[AS^*])\{\xi\} = \bar{U}^2[f^*]_b\{\eta\} \tag{57.23}$$

Fourier transform of Eq. (57.23) yields

$$F(\{\xi\}) = \bar{U}^2[G_1]\{f^*\}_b * F(\{\eta\}) \tag{57.24}$$

where

$$[G_1] = \frac{1}{\left(-\omega^2[M^*] + [K^*] - \bar{U}^2[AS^*] + \omega([D^*] - \bar{U}^2[AD^*])\right)} \tag{57.25}$$

Similarly, taking the conjugate transform of Eq. (57.23) yields

$$\overline{F(\{\xi\})^T} = \bar{U}^2 \overline{F(\{\eta\})^T} \{f^*\}_b^T [G_2]^T \tag{57.26}$$

where

$$[G_2] = \frac{1}{\left(-\omega^2[M^*] + [K]^* - \bar{U}^2[AS^*] - \omega([D^*] - \bar{U}^2[AD^*])\right)} \tag{57.27}$$

The superscript T represents for the matrix transpose, and the overbar stands for the Fourier conjugate transform for the formula above. Multiplying Eqs. (57.24) and (57.26) gives the following spectral density of generalized coordinates

$$\begin{bmatrix} S_{\xi_1\xi_1} & \cdots & S_{\xi_1\xi_m} \\ S_{\xi_i\xi_1} & \cdots & S_{\xi_i\xi_m} \\ S_{\xi_m\xi_1} & \cdots & S_{\xi_m\xi_m} \end{bmatrix} = \bar{U}^4 [G_1] \{f^*\}_b \begin{bmatrix} S_{\eta_1\eta_1} & S_{\eta_1\eta_2} \\ S_{\eta_2\eta_1} & S_{\eta_2\eta_2} \end{bmatrix} \{f^*\}_b^T [G_2]^T \tag{57.28}$$

where $S_{\eta i \eta j}$ = spectral density of normalized wind components. The mean square of the modal and physical displacements can be derived from their spectral densities. Once the displacement is known,

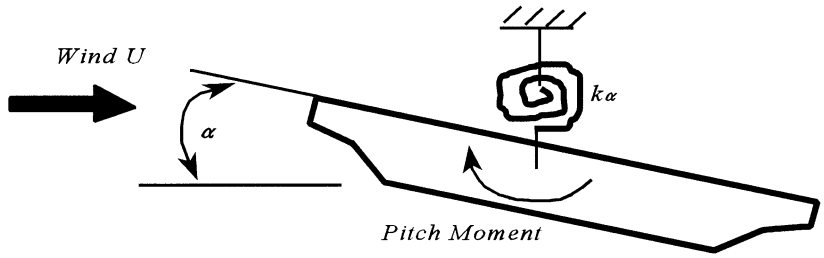

FIGURE 57.6 Explanation of torsional divergence.

the corresponding forces can be derived. The aerodynamic study should ascertain that no structural member is overstressed or overdeformed such that the strength and service limits are exceeded. For very long span bridges, a comfort criterion must be fulfilled under buffeting vibration.

57.4.5 Quasi-Static Divergence

Wind flowing against a structure exerts a pressure proportional to the square of the wind velocity. Wind pressure generally induces both forces and moments in a structure. At a critical wind velocity, the edge-loaded bridge may buckle "out-of-plane" under the action of a drag force or torsionally diverge under a wind-induced moment that increases with a geometric twist angle. In reality, divergence involves an inseparable combination of lateral buckling and torsional divergence.

Consider a small rotation angle as shown in Figure 57.6, the pitch moment resulting from wind is [3]

$$\begin{aligned} M_\alpha &= \frac{1}{2}\,\rho U^2 B^2 C_M(\alpha) \\ &= \frac{1}{2}\,\rho U^2 B^2 \left[C_{M0} + \frac{dC_m}{d\alpha}\Big|_{\alpha=0}\alpha \right] \end{aligned} \tag{57.29}$$

When the pitch moment caused by wind exceeds the resisting torsional capacity, the displacement of the bridge diverges. Equating the aerodynamic force to the internal structural capacity gives

$$k_\alpha \alpha - \frac{1}{2}\,\rho U^2 B^2 \left[C_{M0} + \frac{dC_m}{d\alpha}\Big|_{\alpha=0}\alpha \right] = 0 \tag{57.30}$$

where k_α = spring constant of torsion. For an infinite α, we have the critical wind velocity for torsional divergence as

$$U_{cr} = \sqrt{\frac{2k_\alpha}{\rho B^2 \dfrac{dC_M}{d\alpha}\Big|_{\alpha=0}}} \tag{57.31}$$

57.5 Practical Applications

57.5.1 Wind Climate at Bridge Site

The wind climate at a particular bridge site is usually not available, but it is commonly decided according to the historical wind data of the nearest airport. The wind data are then analyzed

considering the local terrain features of the bridge site to obtain the necessary information such as the maximum wind velocity, dominant direction, turbulence intensity, and wind spectrum. For large bridges, an anemometer can be installed on the site for a few months to get the characteristics of the wind on the site itself. The most important quantity is the maximum wind velocity, which is dependent on the bridge design period.

The bridge design period is decided by considering a balance between cost and safety. For the strength design of a completed bridge, a design period of 50 or 100 years is usually used. Since the construction of a bridge lasts a relatively short period, a 10-year period can be used for construction strength checking. This is equivalent to keeping the same design period but reducing the safety factor during construction.

Flutter is an instability phenomenon. Once it occurs, its probability of failure is assumed to be 100%. A failure probability of 10^{-5} per year for completed bridges represents an acceptable risk, which is equivalent to a design period of 100,000 years. Similarly, the design period of flutter during construction can be reduced to, say, 10,000 years. It should be noted that the design period does not represent the bridge service life, but a level of failure risk.

Once the design period has been decided, the maximum wind velocity is determined. Increasing the design period by one order of magnitude usually raises the wind velocity only by a few percent, depending on the wind characteristics. Wind velocity for flutter (stability) design is usually about 20% larger than that for buffeting (strength) design, although the design period for the former is several orders higher. Once wind characteristics and design velocity are available, a wind tunnel/analytical investigation is conducted.

57.5.2 Design Consideration

The aerodynamic behavior of bridges depends mainly on four parameters: structural form, stiffness, cross section shape and its details, and damping. Any significant changes that may affect these parameters need to be evaluated by a wind specialist.

1. *Structural form*: Suspension bridges, cable-stayed bridges, arch bridges, and truss bridges, due to the increase of rigidity in this order, generally have aerodynamic behaviors from worst to best. A truss-stiffened section, because it blocks less wind, is more favorable than a girder-stiffened one. But a truss-stiffened bridge is generally less stiff in torsion.
2. *Stiffness*: For long-span bridges, it is not economical to add more material to increase the stiffness. However, changing the boundary conditions, such as deck and tower connections in cable-stayed bridges, may significantly improve the stiffness. Cable-stayed bridges with A-shaped or inverted Y-shaped towers have higher torsional frequency than the bridges of H-shaped towers.
3. *Cross section shape and its details*: A streamlined section blocks less wind, thus has better aerodynamic behavior than a bluff section. Small changes in section details may significantly affect the aerodynamic behavior.
4. *Damping*: Concrete bridges have higher damping ratios than steel bridges. Consequently, steel bridges have more wind-induced problems than concrete bridges. An increase of damping can reduce aerodynamic vibration significantly.

Major design parameters are usually determined in the preliminary design stage, and then the aerodynamic behavior is evaluated by a wind specialist. Even if the bridge responds poorly under aerodynamic excitation, it is undesirable to change the major design parameters for reasons of scheduling and funding. The common way to improve its behavior is to change the section details. For example, changing the solid parapet to a half-opened parapet or making some venting slots [8] on the bridge deck may significantly improve the aerodynamic behavior. To have more choices on how to improve the aerodynamic behavior of long-span bridges, to avoid causing delays in the schedule, and to achieve an economical design, aerodynamics should be considered from the beginning.

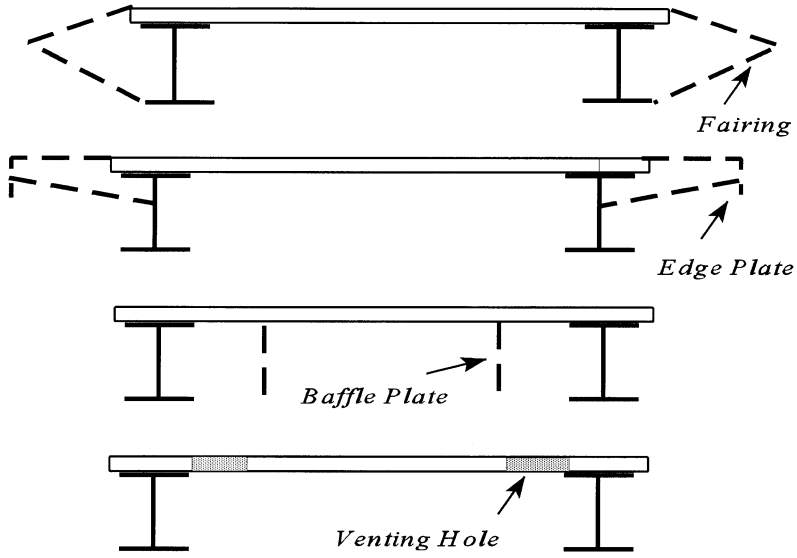

FIGURE 57.7 Typical aerodynamic modifications.

Although a streamlined section is always favorable for aerodynamic behavior, there have recently been many composite designs, due to their construction advantages, for long-span bridges. The composite section shapes, with the concrete deck on steel girders, are bluff and thus not good for aerodynamics, but can be improved by changing section details as shown in Figure 57.7 [9].

57.5.3 Construction Safety

The most common construction method for long-span bridges is segmental (staged) construction, such as balanced cantilever construction of cable-stayed bridges, tie-back construction of arch bridges, and float-in construction of suspended spans. These staged constructions result in different structural configurations during the construction time. Since some construction stages have lower stiffness and natural frequency than the completed bridges, construction stages are often more critical in terms of either strength of structural members or aerodynamic instability.

In the balanced cantilever construction of cable-stayed bridges, three stages are usually identified as critical, as shown in Figure 57.8. They are tower before completion, completed tower, and the stage with a longest cantilever arm. Reliable analytical solutions are not available yet, and wind tunnel testing is usually conducted to ensure safety. Temporary cables, tie-down, and bent are common countermeasures during the construction stages.

57.5.4 Rehabilitation

Aerodynamic design is a relatively new consideration in structural design. Some existing bridges have experienced wind problems because aerodynamic design was not considered in the original design. There are many measures to improve their aerodynamic behavior, such as structural stiffening, section streamlining, and installation of a damper. In the early days, structural stiffening was the major measure for this purpose. For example, the girders of the Golden Gate Bridge were stiffened in the 1950s, and Deer Isle Bridge in Maine has been stiffened since the 1940s by adding stays, cross-bracings, and strengthening the girders [10,11].

Although structural stiffening may have helped existing bridges survive many years of service, section streamlining has been commonly used recently. Streamlining the section is more efficient and less expensive than structural stiffening. Figure 57.9 shows the streamlined section of Deer Isle Bridge which has been proven very efficient [2,10].

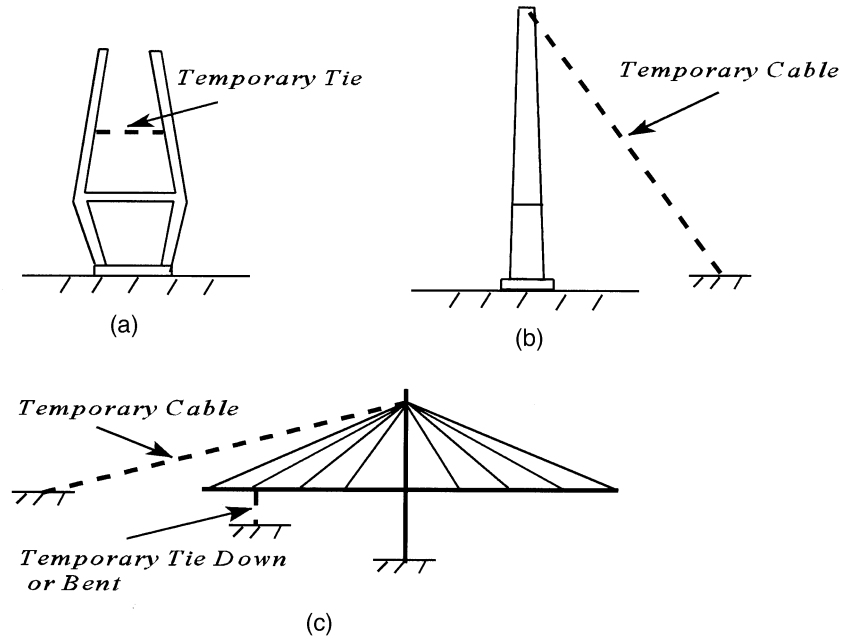

FIGURE 57.8 Typical construction stages. (a) Tower before completion; (b) completed tower; (c) stage with longest cantilever

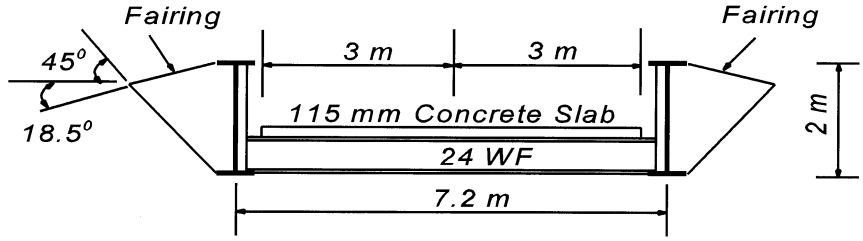

FIGURE 57.9 Deck section and fairings of Deer Isle Bridge.

57.5.5 Cable Vibration

A common wind-induced problem in long-span bridges is cable vibration. There are a number of wind-induced vibrations in cables, individually or as a group, such as vortex excitation, wake galloping, excitation of a cable by imposed movement of its extremities, rain/wind- and ice/wind-induced vibrations and buffeting of cables in strong turbulent winds.

While the causes of the cable vibrations are different from each other and the theoretical solutions complicated, some mitigating measures for these cable vibrations are shared:

1. *Raise damping*: This is an effective way for all kinds of cable vibrations. The cables are usually flexible and inherently low in damping; an addition of relatively small damping (usually at the cable ends) to the cable can dramatically reduce the vibration.
2. *Raise natural frequency*: The natural frequency depends on the cable length, the tension force, and the mass. Since the cable force and the mass are determined from the structural design, commonly the cable length is reduced by using spacers or cross cables.

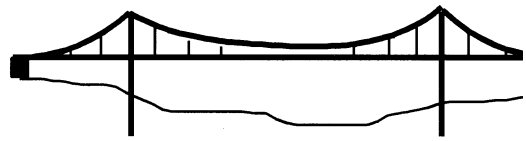

FIGURE 57.10 Explanation of tuned mass damper.

3. *Change cable shape*: A change in the cable shape characteristics by increasing the surface roughness or adding protrusions to the cable surface reduces the rain/wind- and ice/wind-induced vibrations.
4. *Use other techniques*: Rearranging the cables or raising the cable mass density can also be used, but these are usually limited by other design constraints. Raising the mass may reduce the natural frequency, but it increases the damping and Scruton number ($m\zeta/\rho D^2$), and is overall beneficial.

57.5.6 Structural Control

Another way to improve aerodynamic behavior is to install either a passive or active control system on the bridges. A common practice in long-span bridges is the tuned mass damper (TMD). An example is the Normandy cable-stayed bridge in France. This bridge has a main span of 856 m. To reduce the horizontal vibration during construction due to buffeting, a TMD was installed. Wind tunnel testing showed that the TMD reduced the vibration by 30% [12,13].

The basic principles of a passive TMD are explained with an example shown in Figure 57.10. A TMD with spring stiffness k_2 and mass m_2 is attached to a structural mass m_1 which is excited by an external sinusoidal force $F\sin(\omega t)$. The vibration amplitude of this two-mass system is

$$X_1 = \frac{F\omega_m^2\left(\omega_d^2 - \omega^2\right)}{\left(\omega_d^2 - \omega^2\right)\left[\left(k_1 + k_2\right)\omega_m^2 - k_1\omega^2\right] - k_2\omega_d^2\omega_m^2}, \quad X_2 = \frac{F\omega_m^2\omega_d^2}{\left(\omega_d^2 - \omega^2\right)\left[\left(k_1 + k_2\right)\omega_m^2 - k_1\omega^2\right] - k_2\omega_d^2\omega_m^2} \tag{57.32}$$

where $\omega_m^2 = k_1/m_1$ and $\omega_d^2 = k_2/m_2$. It can be seen from Eq. (57.32) that by selection of the stiffness k_2 and mass m_2 such that ω_d equals ω, then the structure vibration X_1 is reduced to zero. Since the wind is not a single-frequency excitation, the TMD can reduce the vibration of bridges, but not to zero.

The performance of the passive TMD system can be enhanced by the addition of an active TMD, which can be done by replacing the passive damper device with a servo actuator system. The basic principle of active TMD is the feedback concept as used in modern control theory.

References

1. Berreby, D., The great bridge controversy, *Discover*, Feb., 26–33, 1992.
2. Cai, C. S., Prediction of Long-Span Bridge Response to Turbulent Wind, Ph.D. dissertation, University of Maryland, College Park, 1993.
3. Simiu, E. and Scanlan, R. H., *Wind Effects on Structures*, John Wiley & Sons, 2nd ed., New York, 1986.
4. Scanlan, R. H., State-of-the-Art Methods for Calculating Flutter, Vortex-Induced, and Buffeting Response of Bridge Structures, Report No. FHWA/RD-80/050, Washington, D.C., 1981.
5. Scruton, C., *An Introduction to Wind Effects on Structures*, Oxford University Press, New York, 1981.
6. Namini, A., Albrecht, P., and Bosch, H., Finite element-based flutter analysis of cable-suspended bridges, *J. Struct. Eng. ASCE*, 118(6), 1509–1526, 1992.

7. Lin, Y. K. and Ariaratnam, S. T., Stability of bridge motion in turbulent winds, *J. Struct. Mech.*, 8(1), 1–15, 1980.
8. Ehsan, F., Jones, N. J., and Scanlan, R. H., Effect of sidewalk vents on bridge response to wind, *J. Struct. Eng. ASCE,* 119(2), 484–504, 1993.
9. Irwin, P. A. and Stone, G. K., Aerodynamic improvements for plate-girder bridges, in *Proceedings, Structures Congress,* ASCE, San Francisco, CA, 1989.
10. Bosch, H. R., A Wind Tunnel Investigation of the Deer Isle-Sedgwick Bridge, Report No. FHWA-RD-87-027, Federal Highway Administration, McLean, VA, 1987.
11. Kumarasena, T., Scanlan, R. H., and Ehsan, F., Wind-induced motions of Deer Isle Bridge, *J. Struct. Eng. ASCE,* 117(11), 3356–3375, 1991.
12. Sorensen, L., The Normandy Bridge, the steel main span, in *Proc. 12th Annual International Bridge Conference,* Pittsburgh, PA, 1995.
13. Montens, S., Gusty wind action on balanced cantilever bridges, in *New Technologies in Structural Engineering,* Lisbon, Portugal, 1997.